# Study on acoustic field with fractal boundary using cellular automata

# Study on Acoustic Field with Fractal Boundary using Cellular Automata

Toshihiko Komatsuzaki[1] and Yoshio Iwata[1]

Graduate School of Natural Science and Technology, Kanazawa University,
Kakuma-machi, Kanazawa, Ishikawa, 920-1192 Japan
{toshi, iwata}@t.kanazawa-u.ac.jp

**Abstract.** In the present study, characteristics of the acoustic field in an enclosure bounded by fractal walls are investigated using Cellular Automata (CA). CA is a discrete system which consists of finite state variables arranged on uniform grid. The dynamics of CA is expressed by temporary updating the states of cells according to the local interaction rules, defined among a cell and its neighbors. In this paper, the effect of fractal shaped boundary structure to the reverberation and sound absorption characteristics of an enclosure is investigated for two dimensional acoustic wave propagation model described by CA. Local rules are provided for the construction of fractal patterns as well as representation of wave propagation phenomena. It is known by the numerical simulations that the damping enhancement and also frequency-selective absorbing behavior is seen for specific fractal patterns and stage numbers.

## 1 Introduction

Among various kinds of sound dissipation schemes, the use of absorptive materials such as porous materials is the most common and significant technique which is widely used for room acoustics and various electric devices. However, the application of such dissipative materials may be limited by their weights, placement and costs. Basically, such absorbing materials can mitigate sound effectively at mid and high frequency range, whereas it is physically well known that they are not much effective for the low frequency regions.

On the other hand, the sound may be reduced by appropriately arranging the acoustic boundary or the sound transmission paths where the sound waves are well diffracted and interfered with each other so that the reverberation characteristic is changed. Several works have been done regarding this issue, where the wave is dissipated depending on the irregularity of the perimeter [2]-[7]. It is also reported that certain acoustic modes are trapped within a part of such irregular boundary which contributes to enhance the damping effect.

The fractal nature would be a measure for evaluating complexity of the boundary.The geometric definition of fractal structure, namely the fractal dimension was first proposed by Mandelbrot in 1975 [1], in order to describe the irregularity of object geometries. The self-similar patterns can be seen in many

natural systems such as in coastlines, clouds, snow flakes and even in economic trends, where the fragments having similar patterns to the whole structures. Typical applications of fractal geometry include artistic designs of computer graphic pictures, engineering applications as the way to analyze spatio-temporal characteristic of images and information. Their intrinsic physical properties are also of general interest and various kinds of researches have also been done with the expectations that any peculiar phenomena may appear due to its self-similarity.

Among many physical processes, the wave responses in fractal structures have been attracted a wide interest and several studies have been done regarding the problem of wave localization in structural vibrations, acoustic waves and electromagnetic waves. The problems of vibrations and acoustic waves within the regions which is bounded by fractal patterns, namely a fractal drum or a fractal cavity were consistently studied by Sapoval et. al [2]-[4]. They have shown analytically that the waves are localized near the perimeter in these surface fractals. They have also shown from more general aspect that the surface irregularities play a role in damping characteristics of the cavity which is contributed by the wave localization. Gibiat et al. have shown specifically for one-dimensional acoustic wave propagation in Cantor-like waveguide that the self-similar structure appears in the frequency response characteristics and that the wave is trapped within such structure [5]. Moreover, the recent work of Kirihara et al.'s have shown experimentally that the incident microwave is confined in the central air cavity of the Menger-sponge fractal by measuring the intensity profile of electric field [7]. The more strong localization of microwaves can also be observed by increasing the fractal stage. As far as the acoustic problems are concerned, such peculiar effects originated by the fractal nature are worth studying with possible application to the room acoustics or the noise control engineering where the reverberation and attenuation characteristics can be controlled. However, the problems may seem rather pattern specific and more extensive research should be done in more effective way for modeling and performing simulations. The Cellular Automata would be a good candidate for that purpose, due to its simplicity but potentiality to express the complex phenomena.

In this paper, both the fractal boundary structure and the acoustic wave model are developed using Cellular Automata (CA), where the acoustic wave propagation is simulated in two dimensional cavity having fractal geometric pattern at the boundary. The wave model is based on past studies by authors where the two dimensional acoustic problems were solved [11, 12]. In the present model, the energy dissipation takes place at the boundary where the wall of the cavity is assumed to be lightly damped without frequency dependence. Response characteristics of fractal patterns which are different in fractal dimension and length of perimeter are compared for the acoustical properties such as the reverberation and dissipation. The effect of the stage number which characterizes the elaborateness of each pattern is also investigated. It is shown that the CA approach is highly compatible with the problems involved. The results also showed that the frequency-selective absorbing behavior is seen for the different fractal patterns and stage numbers, as indicated by the past studies.

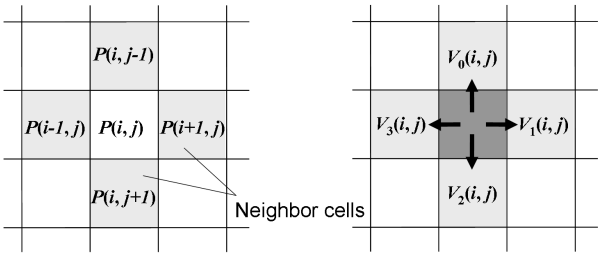


**Fig. 1.** Definition of neighbor in two dimensional acoustic model. Two state variables, sound pressure $P$ and particle velocity $V$, are placed in each cell.

## 2 The Cellular Automata Model for Wave Propagation

Cellular Automata model for simulating acoustic wave propagation is shown in this section. CA has been developed for modeling wide range of phenomena including many physical processes [8]. Specifically the wave propagation models have been studied by researchers based on Cellular Automata [9]-[12]. The simple finite difference scheme obtained by linear wave equation is referenced for developing local interaction rule, in a sense that discretized wave equation yields to an expression of local relationship of wave amplitudes. The rule is then extended to a more practical case, yet time and space are treated as discrete integers. Definitions for state variables and local interaction rules are presented in the following subsections.

### 2.1 Space Partitioning and State Definition

Two dimensional space is discretized into rectangular cells, where state of each cell is distinguished by two integers; i) zero for acoustic media, ii) 1 for lightly absorptive wall. Additionally, two variables which express the sound pressure and particle velocity in four neighbor directions are defined for the acoustic medium state. These variables are updated at each simulation step according to the local interaction rules which describe the relationship between a cell and its cross-located four neighboring cells as shown in Fig.1. Following Cellular Automata convention, time and space are treated as integers. In order for the model to be comparable with actual dimension, we assign unit cell length $dx = 0.001$[m], and also $c = 344$[m/$s$] for sound speed.

### 2.2 Definition of Local Rules

State parameters given in each cell is updated every discrete time step according to a local interaction rule. First, the particle velocities in four directions are updated in time with respect the difference of sound pressure between adjacent cells, whose update rule is described explicitly as,

$$V_a(\mathbf{x}, t+1) = V_a(\mathbf{x}, t) - \{P(\mathbf{x} + \mathbf{dx}_a, t) - P(\mathbf{x}, t)\} \ . \tag{1}$$

$V_a$ represents particle velocity of media and $P$ the sound pressure. Two dimensional cell position is expressed as a vector $\mathbf{x}$ and discrete time step as $t$. A suffix $a$ in (1) signifies index of four neighbors. The particle velocity further obeys the next (2), which expresses linear energy dissipation mechanism.

$$V_a(\mathbf{x}, t) = (1 - n \cdot d) \cdot V_a(\mathbf{x}, t) \ . \tag{2}$$

In the above (2), $n$ represents number of neighbor cells with absorbing wall state, $d$ a damping constant per unit cell. In the present study, $d$ is given as 0.001. The pressure is then updated according to the rule described by (3),

$$P(\mathbf{x}, t+1) = P(\mathbf{x}, t) - c_a^2 \sum_a V_a(\mathbf{x}, t+1) \ , \tag{3}$$

where $c_a$ denotes the wave traveling speed in CA space. Sound pressure and particle velocities are updated according to the local rule described by above three equations.

Since calculation is carried out between nearby cells that are separated only a unit length at every step, any physical quantities cannot have the transport speed exceed to this calculation limit. The maximum wave speed becomes $c_a = 1/\sqrt{2}$ for two dimensional space, therefore the wave front travels $1/\sqrt{2}$ of unit length per calculation step [11].

## 3 Generating Fractal Pattern with CA

The fractal geometries of two dimensional acoustic cavity are produced according to a set of rules within the Cellular Automata framework. Among many patterns that were tested, six fractal patterns which are different in fractal dimension are shown here. The elementary patterns consisting of $5 \times 5$ cells that are used for the boundary construction are shown in Fig.2. The filled square signifies that the cell is a part of wall, and the unfilled a vacant space.

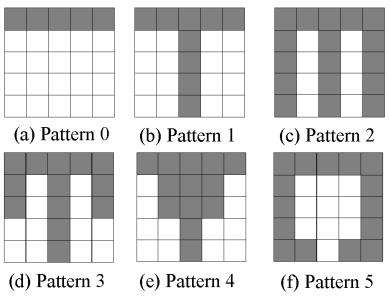


**Fig. 2.** Elementary patterns for generating fractal structure. Fractal dimension of respective pattern is: (a) 1.00, (b) 1.37, (c) 1.76, (d) 1.59, (e) 1.59, and (f) 1.68.

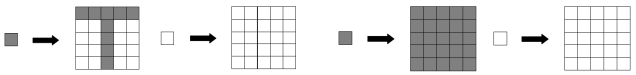

(a) Self-similar pattern growth (b) Enlargement of original pattern

**Fig. 3.** Set of local rules for fractal pattern growth. Rule in (a) generates self-similar pattern according to pre-assigned elementary structure. In (b), a single cell is enlarged to a set of cells having the same state. In both rules a cell is amplified to larger area consisting of $5 \times 5$ grids.

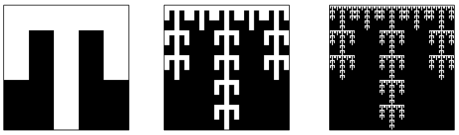

(a) Stage 1 (b) Stage 2 (c) Stage 3

**Fig. 4.** An example of generated $125 \times 125$ cell pattern for respective fractal level based on elementary pattern no. 3.

To generate gross structure of fractal walls with respect to each fractal stage, a set of rules consisting of self-similar growth and enlargement functions should be defined. The self-similar pattern growth rule is used to emphasize elaborateness of fractal pattern, whereas the enlargement rule is applied for simply magnifying the original pattern. These rules are schematically shown in Fig.3. Following each of these rules, a cell is enlarged to a set of cells consisting of $5 \times 5$ grids for single calculation. By combining these rules arbitrarily and calculating for three times, gross structures of $125 \times 125$ cells having fractal geometry will appear corresponding to respective fractal stage number. Examples of fractal picture compared by the stage number varying from stage 1 to 3 for elementary pattern 3 are shown in Fig.4. Starting from a single wall state cell, stage 1 pattern is obtained where the self-similar growth rule is applied once and subsequently the enlargement rule twice. Stage 2 can be calculated by applying the former rule twice followed by latter once. Additionally, stage 3 is obtained by the application of the latter rule three times. It is known from these figures that the self-similar structure is expressed at higher stage numbers.

## 4 Wave Propagation in a Cavity with Fractal Boundary

Simulations are performed for two-dimensional acoustic wave which propagates inside the cavity having fractal geometric patterns developed in Sect.3. Schematic of the acoustic field is shown in Fig.5. The simulation space is divided into $625 \times 625$ cells, where the unit size of a cell is assumed to be 1[mm] which is compatible with physical dimension of $6.25 \times 6.25$[m]. The twelve identical fractal blocks made of $125 \times 125$ cells clusters around the acoustic cavity and constitutes the boundary. A sound source is located at $(130, 130)$, whereas the time history of the sound inside the cavity is observed at $(430, 430)$. Since the choice

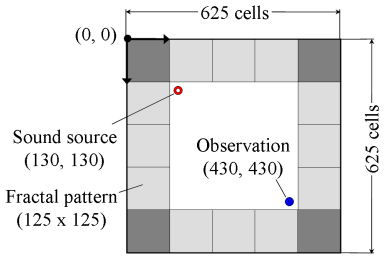


**Fig. 5.** Spatial arrangement of two-dimensional acoustic field.

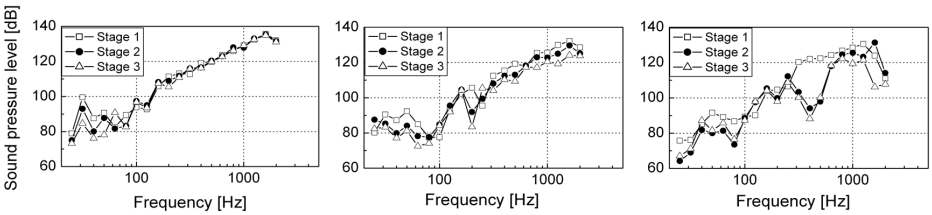


**Fig. 6.** 1/3 octave band sound pressure level of fractal acoustic cavity.

of random excitation is an appropriate way to know the approximate acoustical characteristics of an acoustic field, the white noise filtered with cutoff frequency of 12.5[kHz] is driven by assigning forced particle velocity to the cell. In the following subsections, the gross characteristics regarding reverberation and the damping of sound inside fractal bounded acoustic cavity are shown.

### 4.1 Frequency Response of Sound Pressure Inside Fractal Cavity

While generating random noise, the simulation is carried out for 400,000 iterations which approximately corresponds to the actual time of 8 seconds. Based on the measured time history of the last one second at the observation point, the 1/3 octave band frequency analysis of the sound pressure level for respective fractal boundary pattern is performed. Among six patterns, the frequency responses for the first three patterns are shown in Fig.6. In each pattern the response is also compared by the stage number. As seen from Fig.6(a), the response for pattern 0 where the shape of the perimeter is simply consisted of straight lines is not influenced by the stage sequence, since the geometry is not changed by pattern transformation. The slight change in the pressure level is due to the alteration of the cavity volume. The pressure level is holistically decreased according to the stage number in Fig.6(b) and (c), since the length of perimeter as well as the gross damping effect increases. Also specifically in Fig.6(c), the selective damping enhancement can be seen around 100 and 400[Hz] depending on the stage number. Though it remains conjectural, a certain effect may take place due to the coincidence between the wavelength of sound and the size of concaves in the perimeter. Additionally, the overall sound pressure level for respective fractal

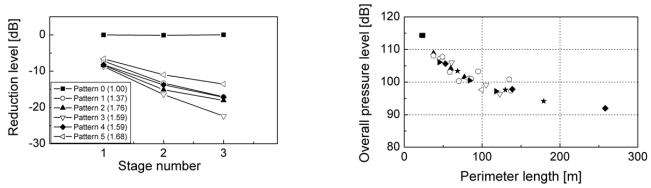


(a) Sound reduction relative to pattern 0 (b) Overall level against perimeter length

**Fig. 7.** Overall sound pressure level.

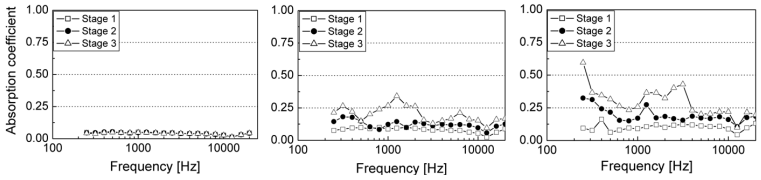


(a) Pattern 0 ($D$=1.00) (b) Pattern 1 ($D$=1.37) (c) Pattern 2 ($D$=1.76)

**Fig. 8.** Absorption coefficient for different boundaries.

pattern is shown in Fig.7. In Fig.7(a), the overall pressure decreases according to the stage development in every pattern. Also it is known that the larger fractal dimension value does not always contribute to larger decrease in overall pressure. Results of all patterns and stages are plotted altogether in Fig.7(b). The figure signifies that the damping of sound pressure inside cavity strongly depends on the length of perimeter, rather than the fractal dimension of elementary pattern.

### 4.2 Equivalent Absorption Coefficient

In order to evaluate the sound dissipation in a room, statistical absorption coefficient is practically derived based on the Eyring's equation [14], written as:

$$T_{\mathrm{r}} = \frac{0.161V}{-S\log_e(1-\alpha)} \ , \tag{4}$$

where the reverberation time $T_{\mathrm{r}}$ is defined as the amount of time in which the sound pressure decreases naturally over time as much as 60dB relative to the pressure when shutting down the source excitation. In (4), $V$ signifies the volume of the cavity and also $S$ the surface area, respectively. Using (4) and measured reverberation time, the absorption coefficient $\alpha$ is reversely calculated for each 1/3 octave band. The sound absorption characteristics for the fractal pattern of 0, 1 and 2 are specifically shown in Fig.8. As easily predicted from Fig.6, significantly low and unchanged absorption characteristic is seen for the acoustic cavity with pattern 0 regardless of the stage number increment. On the other hand, the results of fractal pattern 1 and 2 as in Fig.8(b) and (c) signify that the sound is dissipated as large as the stage number increases. These results imply that even with the limited amount of absorptive treatment on walls, the

sound is effectively damped by providing structural irregularity on the boundary. The frequency-selective behavior must depend on the geometric nature of fractal patterns, which should further be investigated.

## 5 Conclusions

In the present paper, the acoustic wave propagation in a cavity bounded by fractal walls are modeled and investigated using Cellular Automata. Local rules are provided for both the generation of fractal patterns and the representation of wave propagation phenomena. The reverberation and the damping characteristics of the cavity having fractal boundary with different patterns and stages are compared. It is known that the damping of sound inside cavity strongly depends on the length of perimeter, rather than the fractal dimension of elementary pattern. The results also showed that the frequency-selective absorbing behavior is seen for the different fractal patterns and stage numbers. Such pattern specific feature must further be investigated as the future issue.

## References

1. Mandelbrot, B. B.: The Fractal Geometry of Nature. Freeman, San Francisco (1982)
2. Sapoval, B. and Gobron, Th.: Vibrations of strongly irregular or fractal resonators. Phys. Rev. E **47**-5 (1993) 3013–3024
3. Sapoval, B., Haeberle, O. and Russ, S.: Acoustical properties of irregular and fractal cavities. J. Acoust. Soc. Am. **102**-4 (1997) 2014–2019
4. Felix, S., Asch, M., Filoche, M. and Sapoval, B.: Localization and increased damping in irregular acoustic cavities. J. Sound Vib. **299** (2007) 965–976
5. Gibiat, V., Barjau, A., Castor, K. and Chazaud, E. B.: Acoustical propagation in a prefractal waveguide. Phys. Rev. E **67** (2003) 066609
6. Hobiki, Y., Yakubo, K and Nakayama, T.: Spectral characteristics in resonators with fractal boundaries. Phys. Rev. E **54**-2 (1996) 1997–2004
7. Kirihara, S., Takeda M., Sakoda, K. Honda, K. and Miyamoto, Y.: Strong localization of microwave in photonic fractals with Menger-sponge structure. J. Euro. Ceram. Soc. **26** (2006) 1861–1864
8. Chopard, B. and Droz, M.: Cellular Automata Modeling of Physical Systems. Cambridge University Press (1998)
9. Chen, H., Chen, S., Doolen, G., and Lee, Y. C.: Simple Lattice Gas Models for Waves. Complex Systems **2** (1988) 259–267
10. Sudo, Y. and Sparrow, V. W.: Sound Propagation Simulations Using Lattice Gas Methods. AIAA J. **33** (1995) 1582–1589
11. Komatsuzaki, T., Sato, H., Iwata Y. and Morishita, S.: Simulation of Acoustic Wave Propa-gation using Cellular Automata. Trans. JSCES **1** (1999) 135–140
12. Komatsuzaki, T. and Iwata, Y.: Modeling of Sound Absorption by Porous Materials using Cellular Automata. Proc. of 7th International Conference on Cellular Automata for Research and Industry (ACRI2006), LNCS4173 (2006) 357–366
13. Wolfram, S.: A NEW KIND OF SCIENCE. Wolfram Media Inc. (2002)
14. Morse, P. M. and Ingard, K. U.: Theoretical Acoustics. Princeton University Press (1986)